

loss of α diversity. Most important, changes in species composition usually do not result in a substitution of like with like, and can lead to the development of novel ecosystems (19). For example, disturbed coral reefs can be replaced by assemblages dominated by macroalgae (20) or different coral species (21); these novel marine assemblages may not necessarily deliver the same ecosystem services (such as fisheries, tourism, and coastal protection) that were provided by the original coral reef (22).

Our core result—that assemblages are undergoing biodiversity change but not systematic biodiversity loss (Figs. 2 and 3)—does not negate previous findings that many taxa are at risk, or that key habitats and ecosystems are under grave threat. Neither is it inconsistent with an unfolding mass extinction, which occurs at a global scale and over a much longer temporal scale. The changing composition of communities that we document may be driven by many factors, including ongoing climate change and the expanding distributions of invasive and anthropophilic species. The absence of systematic change in temporal α diversity we report here is not a cause for complacency, but rather highlights the need to address changes in assemblage composition, which have been widespread over at least the past 40 years. Robust analyses that acknowledge the complexity and heterogeneity of outcomes at different locations and scales provide the strongest case for policy action. There is a need to expand the focus of research and planning from biodiversity loss to biodiversity change.

References and Notes

- Millennium Ecosystem Assessment, *Ecosystems and Human Well-being: Synthesis* (2006); www.millenniumassessment.org/documents/document.356.aspx.pdf.
- S. H. M. Butchart *et al.*, *Philos. Trans. R. Soc. London Ser. B* **360**, 255–268 (2005).
- J. Loh *et al.*, *Philos. Trans. R. Soc. London Ser. B* **360**, 289–295 (2005).
- B. J. Cardinale *et al.*, *Nature* **486**, 59–67 (2012).
- B. F. Erasmus, S. Freitag, K. J. Gaston, B. H. Erasmus, A. S. van Jaarsveld, *Proc. R. Soc. London Ser. B* **266**, 315–319 (1999).
- S. Ferrier *et al.*, *Bioscience* **54**, 1101–1109 (2004).
- R. H. Whittaker, *Ecol. Monogr.* **30**, 279–338 (1960).
- A. E. Magurran, P. A. Henderson, *Philos. Trans. R. Soc. London Ser. B* **365**, 3611–3620 (2010).
- E. C. Ellis *et al.*, *Proc. Natl. Acad. Sci. U.S.A.* **110**, 7978–7985 (2013).
- A. D. Barnosky *et al.*, *Nature* **471**, 51–57 (2011).
- D. F. Sax, S. D. Gaines, *Trends Ecol. Evol.* **18**, 561–566 (2003).
- M. Vellend *et al.*, *Proc. Natl. Acad. Sci. U.S.A.* **110**, 19456–19459 (2013).
- See supplementary materials on Science Online.
- F. J. Rahel, *Annu. Rev. Ecol. Syst.* **33**, 291–315 (2002).
- C. S. Elton, *The Ecology of Invasion by Animals and Plants* (Univ. of Chicago Press, Chicago, 1958).
- C. Parmesan, *Annu. Rev. Ecol. Syst.* **37**, 637–669 (2006).
- B. Collen *et al.*, *Conserv. Biol.* **23**, 317–327 (2009).
- D. Pauly, *Trends Ecol. Evol.* **10**, 430 (1995).
- R. J. Hobbs *et al.*, *Glob. Ecol. Biogeogr.* **15**, 1–7 (2006).
- T. P. Hughes, *Science* **265**, 1547–1551 (1994).
- J. M. Pandolfi, S. R. Connolly, D. J. Marshall, A. L. Cohen, *Science* **333**, 418–422 (2011).
- N. A. J. Graham, J. E. Cinner, A. V. Norström, M. Nyström, *Curr. Opin. Environ. Sustain.* **7**, 9–14 (2014).

Acknowledgments: Supported by the European Research Council (BioTIME 250189), the Scottish Funding Council (MASTS, grant reference HR09011) (M.D.), and the Royal Society (A.E.M.). We are grateful to all the data providers for making data publicly available and to their funders: Belspo (Belgian Science Policy); NSF; NOAA Marine Fisheries Service (grant NA11NMF4540174); Fisheries and Oceans Canada; Government of Nunavut, Nunavut Wildlife Management Board, Nunavut Tunngavik Inc., and Nunavut Emerging Fisheries Fund; Makivik Corporation; Smithsonian Institution; Atherton Seidell Grant Program; grants BSR-8811902, DEB 9411973, DEB 0080538, DEB 0218039, DEB 0620910, and DEB 0963447 from NSF to the Institute for Tropical Ecosystem Studies, University of Puerto Rico, and to the International Institute of Tropical Forestry, U.S. Forest Service, as part of the Luquillo Long-Term Ecological Research Program; University of Puerto Rico; NSF's Long-Term Ecological Research program and Fishery Administration Agency; Council of Agriculture, Taiwan; Azores Fisheries Observer Program; and the Center of the Institute of Marine Research (IMAR) of the University of the Azores. In addition, data were provided by the H. J. Andrews Experimental Forest research program, funded by NSF's Long-Term Ecological Research Program (DEB 08-23380), P. Henderson (Pisces Conservation), U.S. Forest

Service Pacific Northwest Research Station, and Oregon State University. Cruise data were collected through the logistical efforts of the Australian Antarctic Division and approved by the Australian Antarctic Research Advisory Committee (projects 2208 and 2953), the Australian Antarctic Data Centre of the Australian Antarctic Division, Tasmania. We are also grateful to the databases that compile these data: OBIS, Ecological Data Wiki, DATRAS, and LTER. Finally, we thank O. Mendivil-Ramos for advice on database design, L. Antão, and M. Barbosa and three anonymous referees for comments on earlier versions of the manuscript. The rarefied time series used in our analysis are included as Databases S1 and S2.

Supplementary Materials

www.sciencemag.org/content/344/6181/296/suppl/DC1

Materials and Methods

Figs. S1 to S10

Table S1

Databases S1 and S2

References (23–160)

13 November 2013; accepted 18 March 2014

10.1126/science.1248484

Structural Basis for Assembly and Function of a Heterodimeric Plant Immune Receptor

Simon J. Williams,^{1*†} Kee Hoon Sohn,^{2,6*†} Li Wan,^{1,*} Maud Bernoux,^{3*} Panagiotis F. Sarris,² Cecile Segonzac,^{2,6} Thomas Ve,¹ Yan Ma,² Simon B. Saucet,² Daniel J. Ericsson,^{1†} Lachlan W. Casey,¹ Thierry Lonhienne,¹ Donald J. Winzor,¹ Xiaoxiao Zhang,¹ Anne Coerdts,⁴ Jane E. Parker,⁴ Peter N. Dodds,³ Bostjan Kobe,^{4,5†} Jonathan D. G. Jones^{2†}

Cytoplasmic plant immune receptors recognize specific pathogen effector proteins and initiate effector-triggered immunity. In *Arabidopsis*, the immune receptors RPS4 and RRS1 are both required to activate defense to three different pathogens. We show that RPS4 and RRS1 physically associate. Crystal structures of the N-terminal Toll–interleukin-1 receptor/resistance (TIR) domains of RPS4 and RRS1, individually and as a heterodimeric complex (respectively at 2.05, 1.75, and 2.65 angstrom resolution), reveal a conserved TIR/TIR interaction interface. We show that TIR domain heterodimerization is required to form a functional RRS1/RPS4 effector recognition complex. The RPS4 TIR domain activates effector-independent defense, which is inhibited by the RRS1 TIR domain through the heterodimerization interface. Thus, RPS4 and RRS1 function as a receptor complex in which the two components play distinct roles in recognition and signaling.

Plant immune receptors contain nucleotide-binding and leucine-rich repeat domains and resemble mammalian nucleotide-binding

oligomerization domain (NOD)-like receptor (NLR) proteins (1). During infection, plant NLR proteins activate effector-triggered immunity upon recognition of corresponding pathogen effectors (2, 3). NLR protein activation of defense mechanisms is adenosine triphosphate dependent, causes defense gene induction, and often culminates in the hypersensitive cell death response (hereafter referred to as cell death) (4–6).

In some cases, plant and animal NLRs function in pairs to mediate immune recognition (7). For instance, both *RPS4* (resistance to *Pseudomonas syringae* 4) and *RRS1* (resistance to *Ralstonia solanacearum* 1) NLRs are required in *Arabidopsis* to recognize bacterial effectors AvrRps4 from *P. syringae* pv. *ptisi* and PopP2 from *R. solanacearum* and also the fungal pathogen *Colletotrichum higginsianum* (8, 9). Several NLR gene pairs in rice also function cooperatively to provide resistance to the fungus *Magnaporthe oryzae* (10–14). Similarly,

¹School of Chemistry and Molecular Biosciences and Australian Infectious Diseases Research Centre, University of Queensland, Brisbane, QLD 4072, Australia. ²The Sainsbury Laboratory, John Innes Centre, Norwich Research Park, Norwich, NR4 7UH, UK.

³Commonwealth Scientific and Industrial Research Organisation Plant Industry, Canberra, ACT 2601, Australia. ⁴Max-Planck Institute for Plant Breeding Research, Department of Plant-Microbe Interactions, Carl-von-Linné-Weg 10, D-50829 Cologne, Germany. ⁵Division of Chemistry and Structural Biology, Institute for Molecular Bioscience, University of Queensland, Brisbane, QLD 4072, Australia. ⁶Bioprotection Research Centre, Institute of Agriculture and Environment, Massey University, Private Bag 11222, Palmerston North, 4442, New Zealand.

*These authors contributed equally to this work.

†Corresponding author. E-mail: b.kobe@uq.edu.au (B.K.); jonathan.jones@sainsbury-laboratory.ac.uk (J.D.G.); s.williams8@uq.edu.au (S.J.W.); k.sohn@massey.ac.nz (K.H.S.)

‡Present address: Macromolecular Crystallography, Australian Synchrotron, 800 Blackburn Road, Clayton, Victoria 3168, Australia.

in mammals, the NLR protein NLRC4 acts with either the NLRs NAIP5/6 or NAIP2 to activate defense after recognition of flagellin or bacterial type III secretion rod protein PrgJ, respectively (15). Cooperative activity of immune receptor pairs is thus common in both plants and animals and might operate by evolutionarily conserved mechanisms (16). To address the underlying processes, we investigated how interaction between *Arabidopsis* RPS4 and RRS1 mediates recog-

nition of their corresponding effectors. PopP2, a *Yersinia* YopJ effector family member, is an acetyltransferase that directly interacts with RRS1 in the plant nucleus (17, 18). AvrRps4 is processed in the plant cell, and its C-terminal domain triggers RRS1/RPS4-dependent immunity (19). No direct interaction between AvrRps4 and RRS1 has yet been demonstrated.

RPS4 and RRS1 both carry a Toll–interleukin-1 receptor/resistance protein (TIR) domain at their

N termini. Homo- and heterotypic interactions between TIR domains are implicated in Toll-like receptor signaling pathways in animals, mediating interactions between Toll-like receptors and intracellular TIR domain-containing adaptors to regulate immune signaling and gene expression (20, 21). For several plant TIR-NLR proteins, including RPS4, expression of the TIR domain alone can activate effector-independent defense (22), and for the TIR domain of the flax (*Linum*

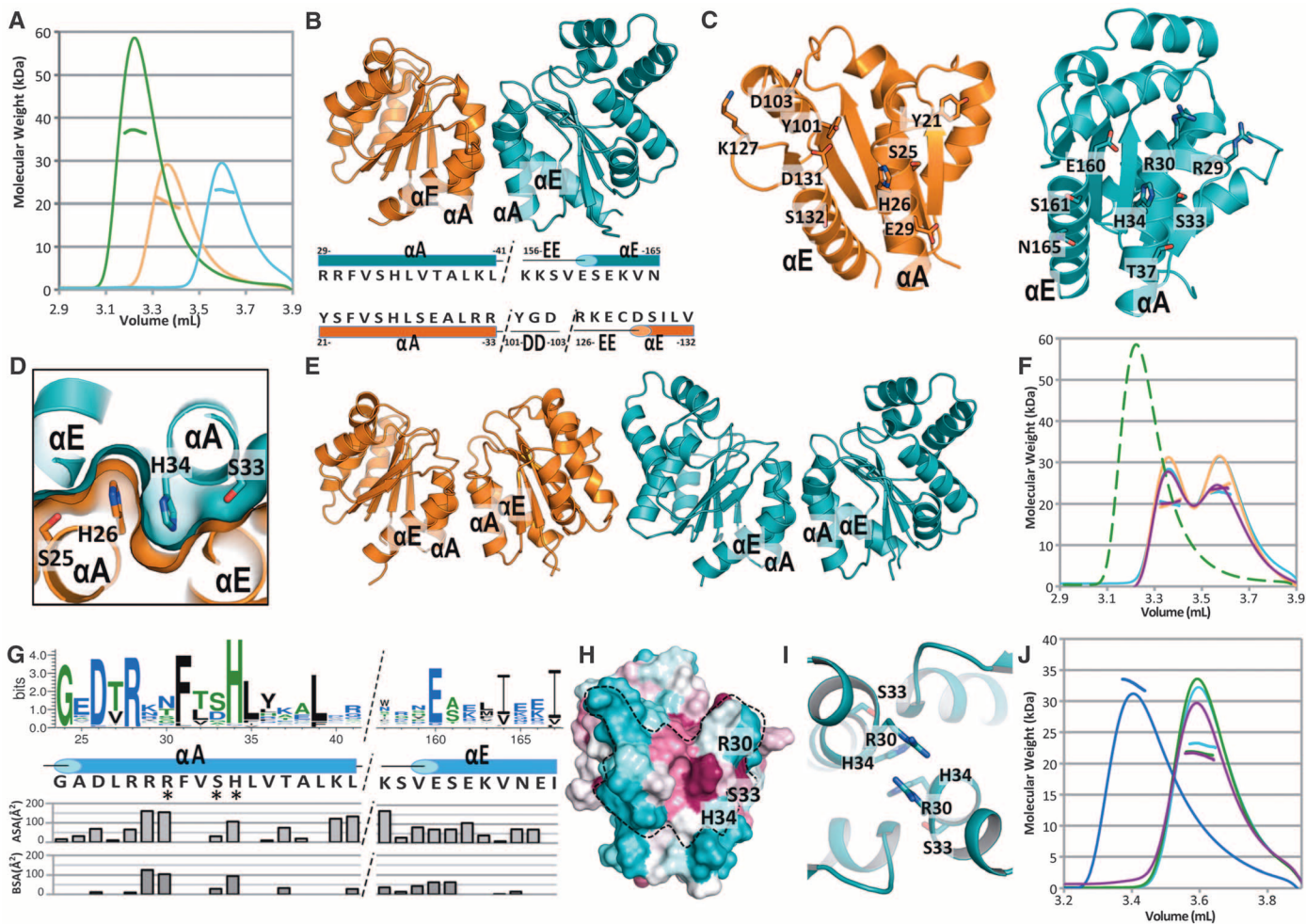


Fig. 1. A conserved TIR/TIR domain interaction interface is involved in hetero- and homo-dimerization between RPS4 and RRS1 TIR domains.

(A) SEC-MALS analysis of RPS4TIR, RRS1TIR, and RPS4TIR + RRS1TIR complex. Green, orange, and teal lines indicate the trace from the refractive index detector (arbitrary units) during SEC of RPS4TIR/RRS1TIR, RRS1TIR, and RPS4TIR, respectively. Solid lines (equivalent coloring) under the peak correspond to the averaged molecular weight (γ axis) distributions across the peak as determined by MALS. (B) Crystal structure of the RRS1TIR (orange) and RPS4TIR (teal) heterodimer shown in cartoon representation. The domains form a pseudosymmetrical dimer with major interactions involving the α A and α E helices of both monomers. Residues contributing to the interface are displayed in the amino acid sequence with secondary structure elements and residue numbers labeled (below). (C) The heterodimerization interface facing the plane of the page. RRS1 and RPS4 rotated -90° and 90° , respectively, around the vertical axis compared to (B), and buried residues are displayed as sticks. (D) The position of serine and histidine residues within the heterodimerization interface. (E) A common interface observed in the crystal packing of RRS1TIR (orange) and

RPS4TIR (teal) structures. (F) Solution properties of SH mutants as measured by SEC-MALS, with traces, units, and calculations represented as for (A). RPS4TIR H34A + RRS1TIR, teal; RPS4TIR + RRS1TIR H26A, orange; RPS4TIR S33A + RRS1TIR S25A, purple. Broken green line represents the refractive index trace of RPS4TIR/RRS1TIR as in (A). (G) Sequence logo (WebLogo 3.3) from a multiple sequence alignment generated by the program ConSurf (34) using 150 unique plant TIR domain sequences (20 to 40% identity to RPS4TIR). Sequence and secondary structure elements of RPS4 are shown below the logo. Asterisks on the sequence represent residues mutated in Fig. 1. Graphs represent residue accessible surface area (ASA) and buried surface area (BSA) within the RPS4TIR structure (\AA^2), calculated by PISA (35). (H) Surface representation of RPS4TIR with coloring by sequence conservation from (G). Cyan and purple corresponds to variable and conserved regions, respectively. Broken black line represents the BSA in the homodimer. (I) Structure of RPS4TIR focusing on the common interface, with labeled residues in stick representation. (J) Solution properties of RPS4TIR mutants measured by SEC-MALS, with traces, units, and calculations represented as for (A). RPS4TIR, teal; H34A, green; S33A, purple; R30A, blue.

usitatissimum) NLR protein L6, homodimerization is involved in defense signaling (23).

We first investigated whether RPS4 and RRS1 TIR domains interact. Using yeast two-hybrid assays (Y2H), we found that although TIR domains of RPS4 and RRS1 self-associate weakly, they interact more strongly with each other and do not interact with L6 or RPP5 TIR domains (fig. S1). We transiently coexpressed RPS4 and RRS1 TIR domains with C-terminal hemagglutinin (HA) or

green fluorescent protein (GFP) tags in *Nicotiana benthamiana* leaves, and coimmunoprecipitation also showed that they weakly self-associate but interact more strongly with each other (fig. S1). The RPS4 TIR (residues 10 to 178, RPS4TIR) and RRS1 TIR (residues 6 to 153, RRS1TIR) domains were then expressed in *Escherichia coli* and purified to homogeneity (see the supplementary materials). RRS1TIR interacts in glutathione *S*-transferase pull-down assays with RPS4TIR

but not with TIR domains from NLR proteins N and L6 (*N. tabacum* and flax, respectively) (fig. S1). Size-exclusion chromatography (SEC) coupled with multiangle light scattering (MALS), as well as small-angle x-ray scattering (SAXS) experiments measured a molecular weight of ~37 kD (Fig. 1A and fig. S2) for the RPS4TIR and RRS1TIR complex, consistent with the formation of a heterodimer. The binding affinity between RRS1TIR with RPS4TIR was estimated to be ~435 nM by isothermal titration calorimetry analysis, which also confirmed a 1:1 binding stoichiometry (fig. S3). By SEC-MALS, the averaged molecular weights of RPS4TIR and RRS1TIR alone were 23 kD and 20 kD (Fig. 1A), respectively, higher than the theoretical monomeric molecular weights of ~20 kD and ~17 kD, and consistent with weak self-association. Thus, the TIR domains of RPS4 and RRS1 form a stable and specific heterodimer but also can self-associate.

To better understand homo- and heterodimerization of RPS4 and RRS1 TIR domains, we crystallized (24) and solved the structures of RPS4TIR and RRS1TIR individually (Fig. 1, B to E, and fig. S4). Covalently linking the protein chains of RPS4TIR and RRS1TIR through a five-residue linker (designated RRS1/RPS4TIR) enabled cocrystallization. The structures of RPS4TIR, RRS1TIR, and RRS1/RPS4TIR were determined at 2.05, 1.75, and 2.65 Å resolution, respectively

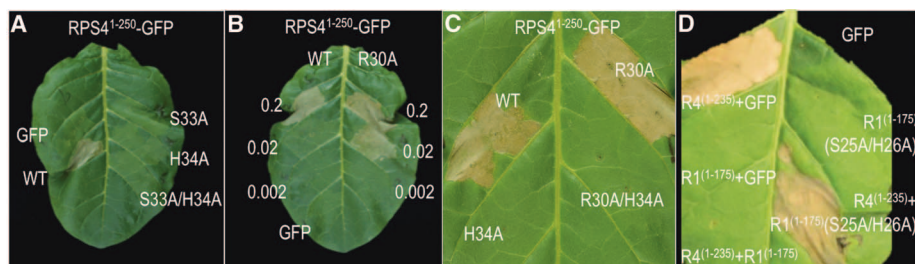


Fig. 2. RPS4 TIR domain–induced cell-death signaling is dependent on the conserved TIR/TIR domain interface. (A) Mutations in the SH motif abolish RPS4 TIR domain–induced hypersensitive response (HR). (B) The R30A mutation enhances HR-inducing activity of RPS4 TIR domain. (C) The H34A mutation abolishes RPS4⁽¹⁻²⁵⁰⁾ TIR domain (R30A)–induced HR. (D) RRS1 TIR domain (R1) suppresses RPS4⁽¹⁻²³⁵⁾ TIR domain (R4)–induced HR. Mutations in the SH motif of RRS1 TIR domain abolish the suppression activity. Agroinfiltration assays were performed in 4- to 5-week-old *N. tabacum* leaves, and images were taken at 2 to 5 days after infiltration. The superscripted numbers in (B) indicate inoculum densities (A_{600}) of *Agrobacterium*.

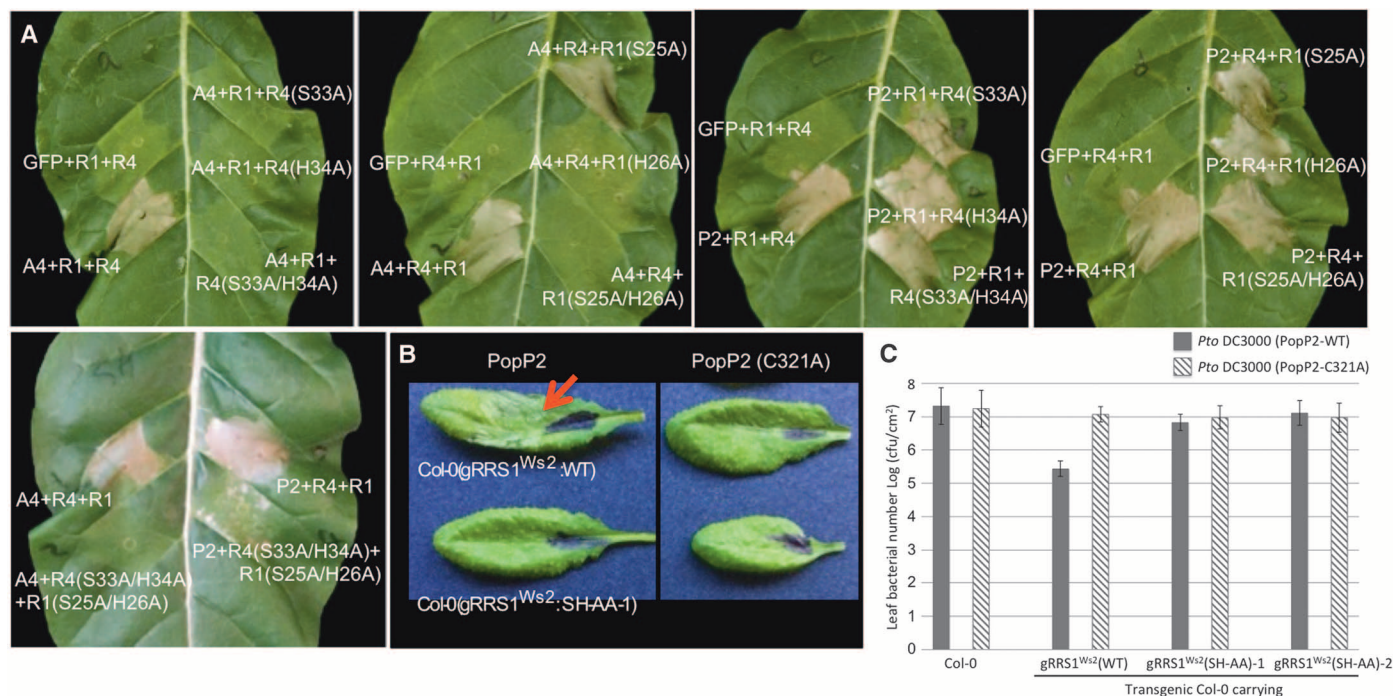


Fig. 3. Mutations that disrupt the RRS1/RPS4 TIR domain dimer abolish the recognition of AvrRps4 and PopP2. (A) The SH motif of RPS4 (R4) and RRS1 (R1) is fully or partially required for recognition of AvrRps4 (A4) or PopP2 (P2), respectively, in *N. tabacum* agroinfiltration assays. The indicated C-terminally epitope-tagged RRS1 (Flag), RPS4 (HA), AvrRps4 (GFP), and PopP2 (GFP) proteins were transiently expressed in *N. tabacum* leaf cells using agroinfiltration. The images were taken at 3 dpi. (B) PopP2-triggered HR is abolished by mutations in the SH motif in the transgenic *Arabidopsis* (Col-0)

line carrying *gRRS1*^{Ws2}. PopP2 variants were delivered from Pf0-1(T3S) into leaves of 5-week-old *Arabidopsis* plants. PopP2^{C321A} represents a catalytic inactive mutant of PopP2 that is not recognized by a resistant RRS1 allele (18). Red arrow indicates HR induced by PopP2. The images were taken at 22 hours after infiltration. This experiment was repeated twice. (C) Transgenically expressed *gRRS1*^{Ws2} carrying SH-AA mutation does not confer resistance to *Pto* DC3000 (PopP2). PopP2 variants were delivered from *Pto* DC3000 and the bacterial colonies were recovered at 4 dpi.

(table S1). The RPS4TIR globular fold comprises a five-stranded parallel β sheet (β A to β E) surrounded by five α -helical regions (α A to α E). In RRS1TIR, the α D-helical region consists of only one helix, in contrast to three observed in RPS4TIR, AtTIR (TIR domain-containing protein AT1G72930 from *A. thaliana*) (25), and L6 TIR domains (23), consistent with a 22-amino acid deletion in RRS1 (fig. S4).

In the RRS1/RPS4TIR crystal, the largest heterodimeric interface involves residues within the α A and α E helices and EE loops of RPS4TIR and RRS1TIR and the DD loop of RRS1TIR (Fig. 1B). This interface is observed twice within the asymmetric unit of the RRS1/RPS4TIR crystal, which consists of two chains of the linked proteins (fig. S5). Surface-exposed residues in RPS4TIR and RRS1TIR contribute to a combined total buried surface area of $\sim 1300 \text{ \AA}^2$ in the heterodimer (Fig. 1C), containing a network of side-chain/side-chain and backbone/side-chain hydrogen bonds (fig. S6). The core of the interface is stabilized by a stacking interaction between histidine residues RPS4 His³⁴ and RRS1 His²⁶ (Fig. 1D). In both proteins, a conserved serine that precedes the histidine within the α A helix forms backbone hydrogen-bonding interactions with a conserved serine in the α E helix of the interacting protein (fig. S6). The adjacent serine and histidine residues (the SH motif) provide complementary stacking and hydrogen-bonding interactions that stabilize the heterodimer (Fig. 1D).

SAXS data were collected on both the RRS1TIR/RPS4TIR heterodimer and the linked (RRS1/

RPS4TIR) construct, and scattering profiles suggested that their behavior in solution was similar (fig. S7). Furthermore, the calculated scattering of the crystallographic dimer was consistent with data from the heterodimer (fig. S7). Thus, the linked RRS1/RPS4TIR protein resembles the heterodimer in solution.

An identical interface to that observed in the RRS1/RPS4TIR heterodimer is also present in the crystal structures of RRS1TIR and RPS4TIR alone (Fig. 1E). The SH motif again forms stacking and hydrogen-bonding interactions; however, the RRS1/RPS4 TIR domain heterodimer interface involves amino acids that are more complementary (fig. S8). This common interface involves different regions of the TIR domain compared to the proposed L6 dimerization interface (23), but an identical interface is observed in the crystal packing of the AtTIR (25) (fig. S9). A multiple sequence alignment of plant TIR domains highlights the conservation of the residues corresponding to Ser³³ and His³⁴ in RPS4 (Fig. 1G). Mapping of this sequence conservation onto the surface of RPS4TIR reveals a patch with the conserved His residue in its center (Fig. 1H).

To investigate the role of specific amino acids in RPS4 and RRS1 TIR domain homo- and heterodimerization, we generated mutations in the interface. In Y2H assays, mutation of residues within the dimeric interface prevents RRS1/RPS4 TIR domain interaction (fig. S10). By SEC-MALS, the most significant effect on heterodimerization is caused by alanine substitutions of the SH motif

(Fig. 1F and fig. S11). Single-residue mutations of the RPS4TIR H34A or RRS1TIR H26A and a double mutation of RPS4TIR S33A/RRS1TIR S25A completely destabilized the TIR/TIR domain heterodimer (Fig. 1F). No interaction could be detected between RRS1TIR and RPS4TIR H34A by isothermal titration calorimetry analysis (fig. S3). Mutation of the SH motif in RPS4 also prevents self-association interactions in Y2H assays (fig. S10). Although weak self-association of wild-type RPS4TIR is observed by SEC-MALS, the S33A and H34A mutants run as monomers (Fig. 1J). Close inspection of the RPS4 TIR domain homodimer interface suggested that the arginine at position 30 likely destabilizes homomeric interactions (Fig. 1I). Mutation of this arginine to an alanine (R30A) results in stronger self-association of RPS4TIR by SEC-MALS (measured $\sim 33 \text{ kD}$) and Y2H assays (Fig. 1J and fig. S10). Sedimentation equilibrium experiments using analytical ultracentrifugation demonstrated that at 15 μM , RPS4TIR R30A completely dimerized, whereas wild-type RPS4TIR formed an equilibrating mixture of monomer and dimer, with an estimated dimerization constant of $13,000 \text{ M}^{-1}$ ($K_d \sim 77 \mu\text{M}$), further corroborating SEC-MALS experiments (fig. S12). Dimerization of RPS4 R30A was only observed when the His³⁴ was maintained (fig. S13).

The TIR domain-containing N-terminal region of RPS4⁽¹⁻²³⁶⁾ activates effector-independent cell death in tobacco (22, 26); this was completely abolished by the S33A, H34A, and S33A/H34A mutations (Fig. 2A and fig. S14). We performed

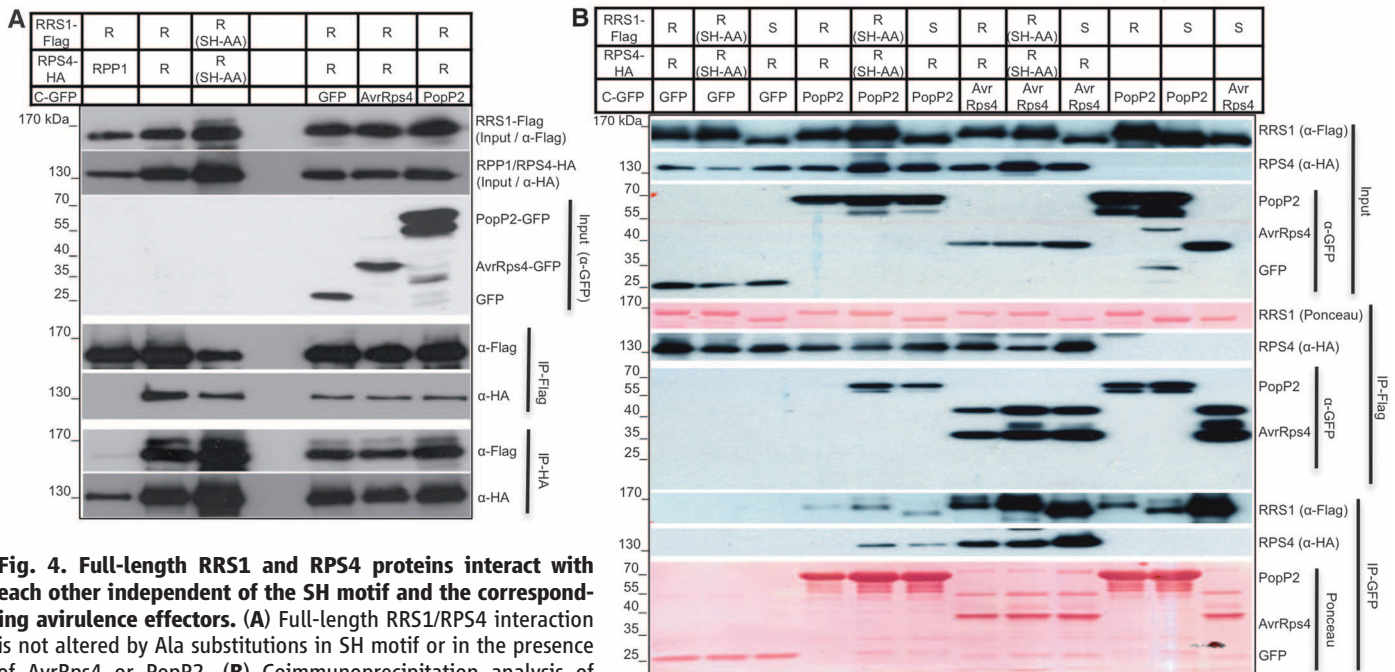


Fig. 4. Full-length RRS1 and RPS4 proteins interact with each other independent of the SH motif and the corresponding avirulence effectors. (A) Full-length RRS1/RPS4 interaction is not altered by Ala substitutions in SH motif or in the presence of AvrRps4 or PopP2. **(B)** Coimmunoprecipitation analysis of RRS1 variants and AvrRps4 or PopP2. The indicated proteins were transiently expressed in *N. benthamiana* leaf cells by agroinfiltration. Total protein extracts were used for coimmunoprecipitation and immunoblot analyzes. R and S indicate resistant and susceptible alleles, in Ws2 and Col-0, respectively, for RRS1. Mutations in the SH motif (SH-AA) have been introduced in RRS1 (Ws-2) and RPS4 (No-0) resistant alleles.

agroinfiltration of serially diluted RPS4 TIR domain and R30A variants in *N. tabacum* leaves. A stronger cell death was induced by the R30A variant than the wild-type protein at 0.02 inoculum density (A_{600}) (Fig. 2B and fig. S14), and the R30A/H34A double mutant was unable to induce cell-death (Fig. 2C), suggesting that homodimerization of RPS4 TIR domain is required for cell death signaling.

Transient expression of RRS1 TIR domain does not cause cell death in *N. tabacum* (Fig. 2D and fig. S14). However, coexpression of RRS1 TIR domain suppressed RPS4 TIR domain-induced cell death, whereas the S25A/H26A loss-of-heterodimerization variant of RRS1 TIR domain did not (Fig. 2D and fig. S14). Because the heterodimeric interaction between RPS4 and RRS1 TIR domains is stronger than homomeric interactions, this suggests that the heterodimer is inactive in signaling and outcompetes the formation of the active RPS4 TIR domain homodimer.

To determine whether the SH motif and TIR/TIR domain heterodimerization are required for effector-triggered immunity, we coexpressed full-length RRS1 and RPS4 with AvrRps4 or PopP2 effectors (or controls) in *N. tabacum* by agroinfiltration (Fig. 3A). Mutations of the conserved histidine and serine/histidine (SH-AA double mutant) in either RPS4 or RRS1 abolished AvrRps4-triggered RRS1/RPS4-dependent cell death. Although these mutations in the individual proteins had little effect on cell death triggered by PopP2, reduced PopP2-triggered immunity was observed when SH-AA mutants of both RPS4 and RRS1 were coexpressed (Fig. 3A). In susceptible *Arabidopsis* (Col-0), transgenically expressed wild-type but not SH-AA mutant RRS1-Ws-2 confers recognition of PopP2 (Fig. 3, B and C, and fig. S15), demonstrating that TIR domain heterodimerization is required to form a functional complex to recognize AvrRps4 and PopP2.

To investigate whether RRS1 and RPS4 proteins interact in planta, we transiently expressed RPS4-HA and RRS1-Flag tag variants, with or without AvrRps4-GFP or PopP2-GFP, in *N. benthamiana* leaves (Fig. 4). The *Arabidopsis* TIR-NLR protein RPP1 (resistance to *Peronospora parasitica* 1) provided a negative control. RPS4-HA, but not RPP1-HA, coimmunoprecipitate with RRS1-Flag (Fig. 4A). SH motif mutations in RPS4 and/or RRS1 TIR domains do not abolish RRS1/RPS4 interactions, suggesting that other domains also contribute to the interaction.

RRS1/RPS4 interaction is independent of the effectors (Fig. 4A). For AvrL567/L6, ATR1/RPP1, and AvrM/M (23, 27, 28), effector/NLR interaction correlates with activation of defense. However, PopP2 interacts in the nucleus with both susceptible (Col-0) and resistant (Nd-1) forms of RRS1 (17). Several other resistant accessions (Ws-2 and No-0) were reported (9, 29). Both RRS1 (Col-0) and RRS1 (Ws-2) coimmunoprecipitate with PopP2 in *N. benthamiana* (Fig. 4B). However, the interactions between PopP2 and RRS1 or RRS1 + RPS4 were stronger in combinations

that do not activate defense [RRS1 (Col-0), RRS1 SH-mutant, PopP2 inactive mutant, or in the absence of RPS4] (Fig. 4B and fig. S16).

AvrRps4 also interacts strongly with RRS1 in the presence or absence of RPS4, and the interaction between RRS1 and AvrRps4 is not affected by an RRS1 SH-AA mutation (Fig. 4B).

Mutations in the P-loop motif of many NLR proteins disturb nucleotide binding and abolish function (4). The RPS4 NB domain P-loop mutation (K242A) abolished recognition of AvrRps4 and PopP2 in transient assays in *N. tabacum* without affecting protein accumulation (figs. S17 and S18). By contrast, an RRS1 P-loop mutation (K185A) did not attenuate AvrRps4 or PopP2-triggered cell death (fig. S18).

Because TIR/TIR domain interactions have previously been difficult to define structurally (30), our data may have broad implications for understanding TIR domain function across phyla. Current models of plant NLR protein activation imply that effector perception leads to considerable domain reorganization and formation of oligomeric forms (31). Rather than effector-induced disassociation of RRS1 and RPS4 proteins, rearrangements within a preformed RRS1/RPS4 complex, culminating in stabilization of an RPS4 TIR domain homodimer, likely distinguish the preactivation complex from its activated state. Domains in RRS1 and RPS4 other than the TIR domain are also likely to hold or bring the complex together and mediate its effector-dependent reconfiguration. Nucleotide-binding or exchange by RPS4, but not RRS1, is required for a functional NLR resistance complex. Thus AvrRps4 or PopP2 recognition is accomplished by an RRS1/RPS4 complex, distinct from indirect recognition of effectors by other plant NLR proteins (32, 33). We propose that upon effector binding, defense activation requires the release of RPS4 TIR domain inhibition by the RRS1 TIR domain, allowing formation of a signaling-competent RPS4 TIR domain homodimer (fig. S19).

References and Notes

- J. L. Dangl, D. M. Horvath, B. J. Staskawicz, *Science* **341**, 746–751 (2013).
- P. N. Dodds *et al.*, *Proc. Natl. Acad. Sci. U.S.A.* **103**, 8888–8893 (2006).
- J. D. G. Jones, J. L. Dangl, *Nature* **444**, 323–329 (2006).
- F. L. Takken, M. Albrecht, W. I. Tameling, *Curr. Opin. Plant Biol.* **9**, 383–390 (2006).
- S. J. Williams *et al.*, *Mol. Plant Microbe Interact.* **24**, 897–906 (2011).
- J. T. Greenberg, *Annu. Rev. Plant Physiol. Plant Mol. Biol.* **48**, 525–545 (1997).
- T. K. Eitas, J. L. Dangl, *Curr. Opin. Plant Biol.* **13**, 472–477 (2010).
- D. Birker *et al.*, *Plant J.* **60**, 602–613 (2009).
- M. Narusaka *et al.*, *Plant J.* **60**, 218–226 (2009).
- I. Ashikawa *et al.*, *Genetics* **180**, 2267–2276 (2008).
- S. Cesari *et al.*, *Plant Cell* **25**, 1463–1481 (2013).
- S.-K. Lee *et al.*, *Genetics* **181**, 1627–1638 (2009).
- Y. Okuyama *et al.*, *Plant J.* **66**, 467–479 (2011).
- B. Yuan *et al.*, *Theor. Appl. Genet.* **122**, 1017–1028 (2011).
- E. M. Kofoed, R. E. Vance, *Nature* **477**, 592–595 (2011).
- J. von Moltke, J. S. Ayres, E. M. Kofoed, J. Chavarría-Smith, R. E. Vance, *Annu. Rev. Immunol.* **31**, 73–106 (2013).
- L. Deslandes *et al.*, *Proc. Natl. Acad. Sci. U.S.A.* **100**, 8024–8029 (2003).
- C. Tasset *et al.*, *PLoS Pathog.* **6**, e1001202 (2010).
- K. H. Sohn, Y. Zhang, J. D. G. Jones, *Plant J.* **57**, 1079–1091 (2009).
- K. Takeda, S. Akira, *Int. Immunol.* **17**, 1–14 (2005).
- T. Ve, N. J. Gay, A. Mansell, B. Kobe, S. Kellie, *Curr. Drug Targets* **13**, 1360–1374 (2012).
- M. R. Swiderski, D. Birker, J. D. G. Jones, *Mol. Plant Microbe Interact.* **22**, 157–165 (2009).
- M. Bernoux *et al.*, *Cell Host Microbe* **9**, 200–211 (2011).
- L. Wan *et al.*, *Acta Crystallogr. Sect. F Struct. Biol. Cryst. Commun.* **69**, 1275–1280 (2013).
- S. L. Chan, T. Mukasa, E. Santelli, L. Y. Low, J. Pascual, *Protein Sci.* **19**, 155–161 (2010).
- Y. Zhang, S. Dorey, M. Swiderski, J. D. Jones, *Plant J.* **40**, 213–224 (2004).
- K. V. Krasileva, D. Dahlbeck, B. J. Staskawicz, *Plant Cell* **22**, 2444–2458 (2010).
- T. Ve *et al.*, *Proc. Natl. Acad. Sci. U.S.A.* **110**, 17594–17599 (2013).
- Y. Noutoshi *et al.*, *Plant J.* **43**, 873–888 (2005).
- E. Valkov *et al.*, *Proc. Natl. Acad. Sci. U.S.A.* **108**, 14879–14884 (2011).
- F. L. Takken, A. Goverse, *Curr. Opin. Plant Biol.* **15**, 375–384 (2012).
- M. J. Axtell, B. J. Staskawicz, *Cell* **112**, 369–377 (2003).
- D. Mackey, Y. Belkadir, J. M. Alonso, J. R. Ecker, J. L. Dangl, *Cell* **112**, 379–389 (2003).
- H. Ashkenazy, E. Erez, E. Martz, T. Pupko, N. Ben-Tal, *Nucleic Acids Res.* **38**, (Web Server), W529–W533 (2010).
- E. Krissinel, K. Henrick, *J. Mol. Biol.* **372**, 774–797 (2007).

Acknowledgments: This research was supported by the Australian Research Council (ARC) Discovery Project (DP120100685), by Rural Development Administration (Korea) Project PJ007850201006, and by the Gatsby Foundation (United Kingdom). M.B. was a recipient of an ARC Discovery Early Career Award (DE130101292). A.C. is an International Max-Planck Research School Ph.D. student. B.K. is a National Health and Medical Research Council Research Fellow (1003325). P.F.S. is supported by the European Commission FP7-PEOPLE-2011-Intra-European Fellowships (299621). The x-ray diffraction and small-angle scattering data collection was undertaken on the Micro Crystallography and Small- and Wide-Angle X-Ray Scattering beamlines at the Australian Synchrotron. We thank the Australian Synchrotron beamline scientists for help with x-ray data collection, and we acknowledge the use of the University of Queensland Remote Operation Crystallization and X-ray Diffraction Facility (UQ ROX). We thank R. Counago for valuable help and suggestions, K. Newell and J. Rajamony for providing excellent technical assistance, Icon Genetics and S. Marillonnet for early access to vectors, and J. Ellis and S. Cesari for critical reading of the manuscript. The coordinate and structure factor data for RPS4TIR, RRS1TIR, and RRS1/RPS4TIR have been deposited to the Protein Data Bank (PDB) with PDB IDs 4c6f, 4c6s, and 4c6t, respectively.

Supplementary Materials

www.sciencemag.org/content/344/6181/299/suppl/DC1
Materials and Methods
Supplementary Text
Figs. S1 to S19
Table S1
References (36–64)

18 October 2013; accepted 12 March 2014
10.1126/science.1247357



Structural Basis for Assembly and Function of a Heterodimeric Plant Immune Receptor

Simon J. Williams *et al.*
Science **344**, 299 (2014);
DOI: 10.1126/science.1247357

This copy is for your personal, non-commercial use only.

If you wish to distribute this article to others, you can order high-quality copies for your colleagues, clients, or customers by [clicking here](#).

Permission to republish or repurpose articles or portions of articles can be obtained by following the guidelines [here](#).

The following resources related to this article are available online at www.sciencemag.org (this information is current as of March 6, 2016):

Updated information and services, including high-resolution figures, can be found in the online version of this article at:

</content/344/6181/299.full.html>

Supporting Online Material can be found at:

</content/suppl/2014/04/16/344.6181.299.DC1.html>

A list of selected additional articles on the Science Web sites **related to this article** can be found at:

</content/344/6181/299.full.html#related>

This article **cites 64 articles**, 17 of which can be accessed free:

</content/344/6181/299.full.html#ref-list-1>

This article has been **cited by** 11 articles hosted by HighWire Press; see:

</content/344/6181/299.full.html#related-urls>

This article appears in the following **subject collections**:

Botany

</cgi/collection/botany>